Textures and Microstructures, 1988, Vols. 8 & 9, pp. 531–549
Reprints available directly from the publisher
Photocopying permitted by license only

Printed in the United Kingdom

Grain-Specific Texture Measurements

VALERIE RANDLE and BRIAN RALPH
Department of Materials Technology, Brunel University, Uxbridge, UK

(Received 30 August 1987)

Dedicated to the memory of Professor Günter Wassermann

In order to obtain the fullest possible picture of the interrelationship between texture, microstructure and properties it is necessary to collate data on a "micro-textural" (i.e. grain specific) basis, in addition to more conventional macrotexture measurements. This paper describes two methods for the acquisition of microtextural data, the electron backscattering diffraction technique in a scanning electron microscope, and convergent beam electron diffraction in a transmission electron microscope. The former method is particularly suitable for the collection of large quantities of data, and examples of its use are included. In addition to an inverse pole figure presentation of texture, orientation measurements which arise from contiguous grains may be analysed from the standpoint of the grain misorientation texture (GMT). From this type of microtextural data the proportion and distribution of grain boundaries which possess special properties can be obtained. Since it has recently been recognised that the properties of special boundaries have a significant influence on the overall properties of the material, the ability to collect and analyse easily such data in statistically significant quantities represents an extremely powerful research technique. Finally, a method for computer generation of GMTs, both from randomly oriented and textured grain aggregates is described and compared with the experimental case.

KEY WORDS: Electron backscattering diffraction, convergent beam electron diffraction, inverse pole figure, grain misorientation texture, grain size classes, special boundaries.

INTRODUCTION

The texture of a polycrystalline aggregate has a significant influence on its properties and extremely sophisticated techniques have been

developed for measuring and representing macrotexture (e.g. inverse pole figures and orientation distribution functions). Further, measurements of the evolution of texture components give very considerable insight into the mechanisms occurring during the thermomechanical processing of materials (e.g. Bunge, 1982; Hatherley and Hutchinson, 1979). An example of this comes from recent studies of texture development accompanying various forms of grain growth (e.g. Bunge and Dahlem, 1986) where it may be shown that anomalous grain growth may be associated with particularly texture-type modifications (e.g. Abbruzzese and Lücke, 1986).

In such studies it may be possible to infer some relationship between grain boundary structure/properties and the texture or a texture change. However, to obtain a fuller picture of the interrelationship between texture, microstructure and properties really requires the texture to be obtained on a grain specific basis. Hitherto, obtaining such "microstructural" data has been either difficult or extremely time consuming. Most of the basic studies on bicrystals have made use of Laue X-ray techniques which can be extended to coarse grained polycrystals (e.g. Inoko, 1986). Other studies have involved the use of electron channelling and the Kossel technique in a scanning electron microscope, SEM (e.g. Grant *et al.*, 1986) and at a finer scale level electron diffraction in a transmission electron microscope, TEM, has been used to establish a full description of the grain boundary geometry. The sample size for studies by TEM is rather small but the advent of convergent beam electron diffraction, CBED, techniques, has permitted relatively accurate data to be acquired relatively efficiently (e.g. Randle and Ralph, 1986a).

Where a strong texture is present, it is frequently observed that the grain boundaries reflect this by the occurrence of a high proportion of boundaries misoriented about a common axis. For example, a wire of a cubic metal with a strong $\langle 100 \rangle$ fibre texture gives rise to many boundaries misoriented about $\langle 100 \rangle$ (e.g. Howell *et al.*, 1978). Furthermore a high proportion of geometrically special boundaries such as those of low angle type and coincidence site lattice (CSL) boundaries misoriented about the fibre axis would also be strongly favoured. Where the texture is less pronounced it becomes less apparent if the proportion and distribution of geometrically special boundaries may be attributed to the grain texture

(Pumphrey, 1976). In fact, the grain boundary distribution itself may display a texture. The present authors call this the "grain misorientation texture" (GMT) because it refers to the misorientation between grains (as distinct from the orientation of the boundary plane) (e.g. Dechamps *et al.*, 1985).

A microtextural instead of a macrotextural approach then allows access to two kinds of orientational information. Firstly the texture of individual grains may be identified and any correlation with grain size or other parameters (e.g. residual strains, particle/solute distribution, surface energies) assessed. Secondly where the measurements arise from contiguous grains GMT data, including proportions and distributions of special boundaries, becomes available. Knowledge of the latter is of particular relevance to the control of material properties and behaviour. This relatively new area of materials science has been termed "grain boundary engineering" by Watanabe (Watanabe, 1984; Sickafus and Sass, 1987; Randle and Ralph, 1987a). The basis of the grain boundary engineering concept is that special grain boundaries possess properties which may be beneficial to the overall properties of materials, such as strength, fracture toughness, ductility and corrosion resistance. Here a distinction must be drawn between boundaries that are special in a geometrical sense (usually taken to mean low angle and CSL boundaries up to about $\Sigma = 29$) insofar as they have a periodic, ordered structure and boundaries which have special properties (i.e. markedly different from the properties of an average random boundary). Most boundaries which have been found to have special properties are also geometrically special; however the latter is not necessarily true. This point is discussed in more detail later.

The eventual aim then is to design materials which feature a high proportion of the required boundaries. The first steps towards this ideal must therefore be to characterise thoroughly GMTs for a variety of heat treatment and microstructural conditions. By use of a newly available experimental technique (electron back scattering, EBS, in a scanning electron microscope (e.g. Dingley, 1984; Randle *et al.*, 1987) and convergent beam electron diffraction in a transmission electron microscope, the authors are compiling and analysing a large data base of microtextural and GMT information for several materials. Particular emphasis is being placed on monitoring shifts in the grain boundary character distribution as a function of heat

treatment and collating the microtexture with the GMT for specific regions of specimens. In this paper the methods for obtaining and presenting microtextural/GMT data will be described and some of the experimental data reviewed. Finally a computer simulation approach to GMT is described and compared to the experimentally obtained data.

EXPERIMENTAL TECHNIQUES

The electron back scattering method

The electron back scattering method relies on the principle that when an electron beam impinges upon a specimen, part of the signal is absorbed and the remainder is diffracted at the specimen surface. By tilting the specimen so that the incident beam makes a small angle with the specimen surface (Figure 1) most of the signal is back scattered rather than absorbed. Dingley (1984) has exploited this phenomenon using a configuration shown in Figure 1 and the resulting system may be used quite routinely to measure microtextures from regions of specimen down to sub-micrometre size. External software allows the operator to obtain an orientation in about one minute. Grain misorientations may also be computed. The procedure is described in more detail elsewhere (Dingley, 1984;

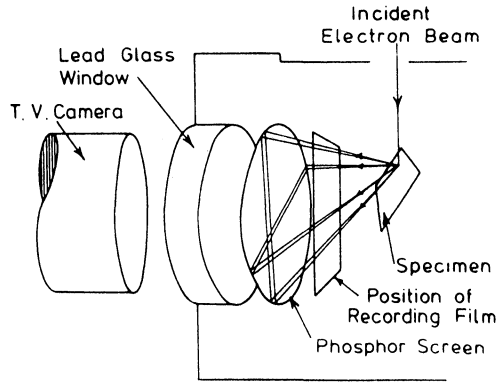

Figure 1 Schematic diagram to illustrate the layout of the EBS equipment.

Table 1 Comparison of the EBS/SEM method of grain boundary structural analysis with the CBED/TEM method

EBS	CBED
Accuracy for measurement of l/θ 1–2°.	Accuracy for measurement of l/θ 0.5°
Data analysis on-line and semi-automatic, therefore very rapid	Data handling under operator control from diffraction patterns therefore slower
Many hundreds of grain boundaries available in a single sample	Typically 20–30 boundaries available in a single foil
The grain size distribution can be analysed in terms of grain microtexture and related to the GMT	No grain size specific information
Information available restricted to that pertaining to grain orientations	Grain boundary planes, dislocation characters and atomic level composition profiles can be determined

Randle *et al.*, 1987). Examples of data obtained by this method are included in the following main section (Results).

The convergent beam electron diffraction method

Convergent beam electron diffraction may be applied in a TEM to obtain axis/angle pair data and subsequently processed to obtain GMTs (Randle & Ralph 1985, 1986a). A portion of the experimental results which are reviewed in the results section have been obtained by this method. Table 1 compares the CBED method of obtaining microtextural/GMT information with the EBS route. For application to large sets of data (typically hundreds of boundaries) EBS is clearly preferable to CBED in terms of speed, and an accuracy of $\pm 1°$ for the grain misorientations would be acceptable in these circumstances. For purposes of comparison the exact misorientation of an incoherent twin boundary in a thin foil specimen of a nickel-based super-alloy Nimonic PE16 was first obtained by CBED and then by EBS: the axis/angle of misorientation thus obtained was 590 585 555/58.3° and 593 577 561/59·4° respectively, which demonstrates an adequate agreement between the two techniques and an expected 111/60° result.

For certain circumstances, however, CBED may be the more favourable technique or alternatively could be used in conjunction

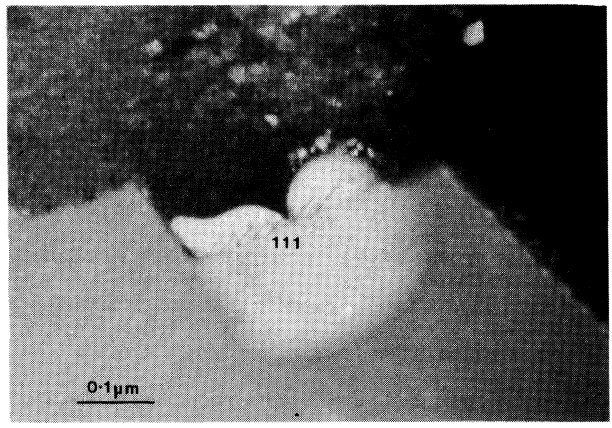

Figure 2 (111) facet of twin boundary cutting through a coherent γ' precipitate in Nimonic PE16. The other boundary facet type, which is near to (112), does not cut through precipitates, thus illustrating a dependence of boundary properties on the orientation of the boundary plane.

with EBS. These circumstances include investigations where it is necessary to have access to grain bounday parameters which are only available through TEM, such as boundary segregation profiles, defect structure, intergrangular precipitate nucleation and growth, and the orientation of the boundary plane. Situations may arise where the boundary plane orientations are textured, such as in the case of "two dimensional" materials where the sheet thickness is less than the grain size. Boundary plane texture is significant since the properties of special boundaries are boundary plane orientation specific. An example is shown in Figure 2—which shows a coherent γ' precipitate being cut by the (111) facet of a twin boundary. The other boundary facet, which is near (112), does not cut through precipitates. This is a common feature in this alloy. Here the plane orientation was obtained by a CBED method which includes measuring the foil thickness, and a stereographic procedure.

RESULTS

The results which will be presented here are from Nimonic PE16 rod stock and have all arisen as part of a study of the factors which

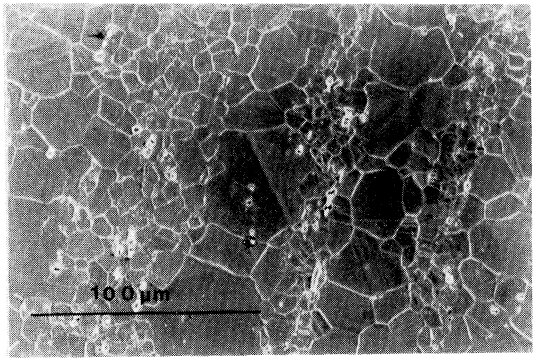

Figure 3 The "banded" dual-size grain structure of Nimonic PE16, where columns of large grains are interspersed with smaller grains.

influence grain growth, and in particular anomalous grain growth (Randle and Ralph, 1987a; Randle and Ralph 1987b; Randle *et al.*, 1987).

Anomalous grain distributions

The microstructure of PE16 tends to be inhomogeneous. One manifestation of this non-uniformity is the commonly observed banded grain structure, which features columns of large grains interspersed with smaller grains (Figure 3). Macroscopic texture measurements indicate a relatively random texture for this material; however EBS measurements are able to provide microtextural data from the large and small grains on a size basis. Figure 4 shows inverse pole figures from the longitudinal direction (parallel to the rod axis) which clearly show the dual nature of the texture, with only small grains predominating in the ⟨001⟩ and ⟨111⟩ regions of the unit stereographic triangle (*a*-type texture) and large grains having their orientations nearer the triangle centre (*b*-type texture).

As an alternative to the banded structure the irregular grains structure of PE16 may manifest itself as isolated large grains, or small groups of large grains randomly dispersed throughout a matrix of small grains. The microtexture for fifteen grain "assemblies" (i.e. one large grain plus the small grains which surround it) was measured. The results indicate that the longitudinal direction

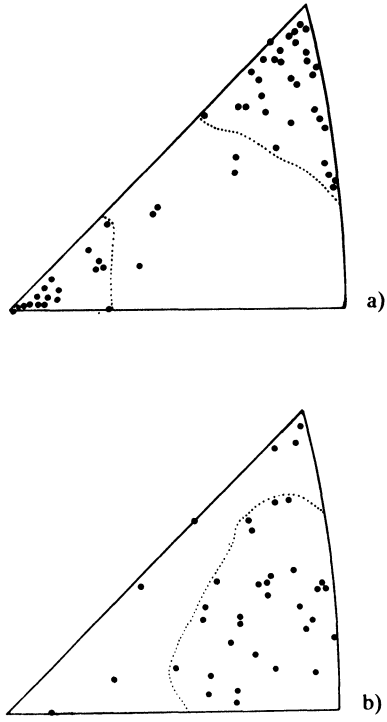

Figure 4 Inverse pole figures in the longitudinal specimen direction (i.e. parallel to the longitudinal axis of the bar) from a) the small grained region and b) the large grained region.

inverse pole figures from each assembly possessed either an *a*-type or a *b*-type texture, and the summation of both the pole figures is shown in Figure 5. The *a*-texture may be considered to be a 'hard' texture, and conversely the *b*-texture contains only 'soft' orientations (Honeycombe, 1982). Often both these texture types occurred in the same specimen, and so would not have been revealed by macro-texture measurements. The hard/soft explanation for the observed microtextures is further substantiated by further annealing a specimen, whereupon an *a*-texture assembly changed to a *b*-texture. Very little grain growth accompanies this texture change.

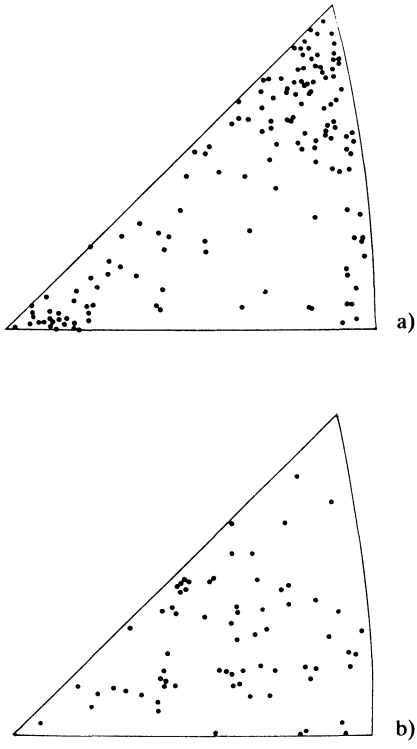

Figure 5 *a*- and *b*-type inverse pole figures from fifteen grain assemblies in PE16.

Grain misorientation textures (GMT)

Grain boundaries which comprise the grain assemblies may be categorised according to whether they interface a large grain with a small grain (LS boundaries) or two small grains (SS boundaries). The GMTs for both these groups are shown in Figure 6. The density contours for a random distributuion of misorientation axes are reproduced on Figure 6 (Mackenzie, 1964) so that they may be compared to the experimental case; a student's *t*-test (Ractliffe, 1967) reveals that both distributions are non-random, and furthermore the SS boundaries are less randomly distributed than the LS types.

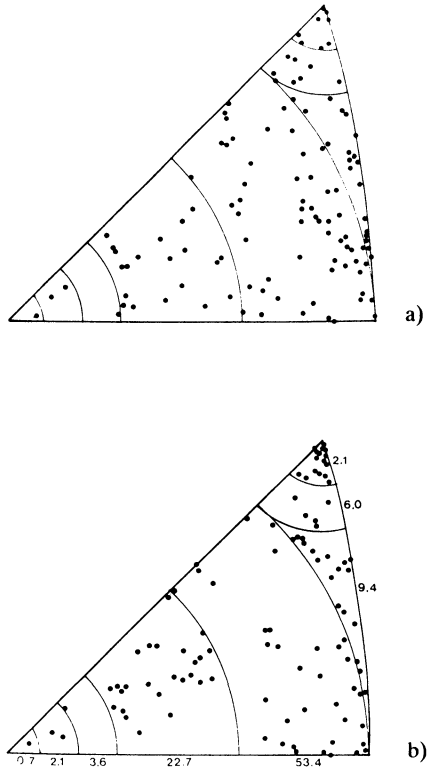

Figure 6 GMTs for a) grain boundaries between large and small grains (LS); and b) boundaries between small grains (SS). Density contours for a random distribution are included on this figure.

The GMT plot alone gives only information pertaining to the distribution of misorientation axes. The angle of misorientation is also required in order to assess if a boundary is special or random. Table 2 shows the proportions of CSLs and low angle boundaries for both SS and LS boundaries. The information is displayed in more detail in Figure 7 where boundaries are categorised according to their proximity to exact CSL matching (v/v_m) and their axis of misorientation and Σ value. Boundaries which have special properties are considered to be the following combinations of Σ and boundary plane: Σ3(111), (110) and (211), Σ11(311), Σ19a(331)

Table 2 Proportions of non-random boundaries between small/small grains (SS) and large/small grains (LS) (%) in a grain assembly consisting of a single large grain surrounded by small grains

	CSL (including $\Sigma = 3$)	Low angle ($<10°$)	$\Sigma = 3$, % of CSL	CSL $<0.5v/v_m$ only
SS	34	12	59	13
LS	30	5	48	6

v is angular deviation from exact CSL.
v_m is maximum allowed angular deviation from a CSL.

Σ5(210), Σ27a(551) and Σ9(221) (full, large symbols on Figure 7), and to a lesser extent, six other CSLs (open symbols) on Figure 7 (Bouchet and Priester, 1987). The information contained in Figure 7 and Table 2 conveys firstly that for both SS and LS groups most CSLs are these types which give rise to special boundary properties (if it is assumed that the grain boundary planes are those listed above) and secondly, the SS group contains a higher proportion of special boundaries, and its CSLs tend towards lower values of v/v_m (i.e. closer to exact CSLs) than the LS group. These results have been interpreted in terms of the accumulation of solute plus the geometrical constraints imposed by the co-existance of large and small grains (Randle and Ralph, 1987b).

Effects of precipitation on the Grain Misorientation Texture

A limited proportion of the PE16 microtexture/GMT work has been performed by use of CBED, as described in a previous section. Here data was obtained from (1) fully aged PE16, where the boundaries were pinned by γ' precipitates; (2) overaged specimens where the strong pinning had prevented boundary migration; and (3) overaged plus solution treated specimens where the strongly pinned grain boundaries in (2) were allowed to migrate when γ' dissolved during the heat treatment. During these stages the GMT altered, as shown on Figure 8 (Randle and Ralph, 1987a and Table 3). The most striking change is the correlation between the CSL fraction and the duration of boundary pinning, with 50% of boundaries in the overaged set found to be CSLs ($\Sigma \leqslant 49$).

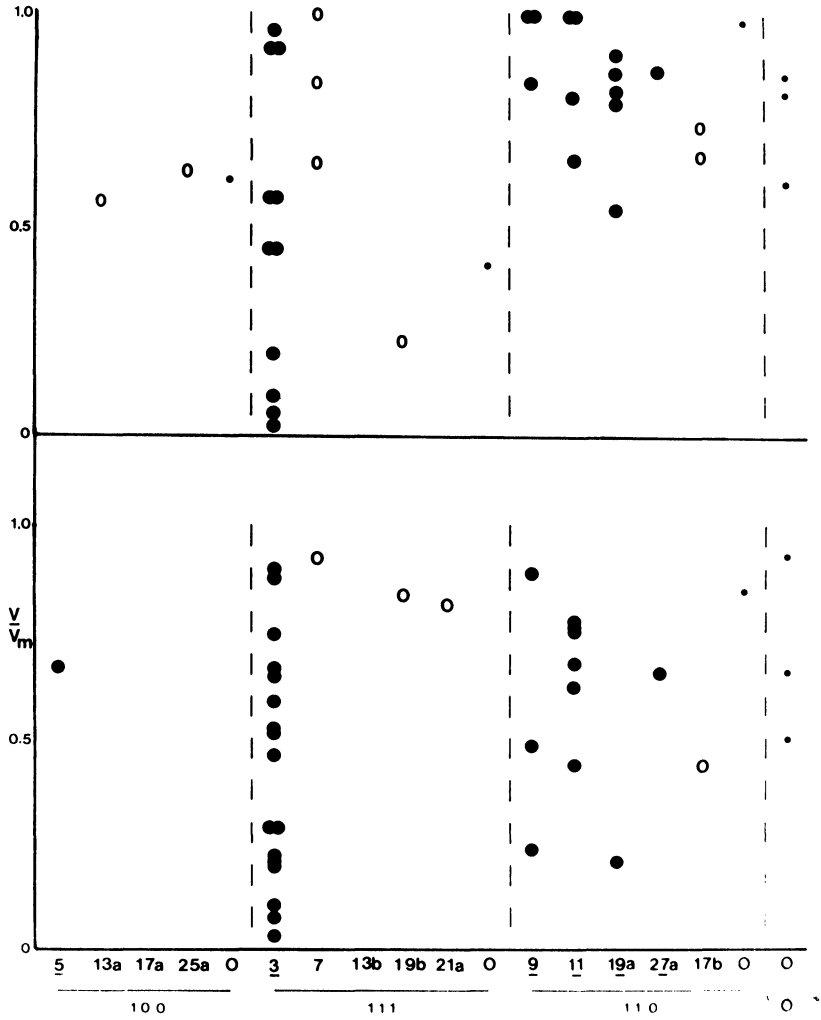

Figure 7 Categorisation of LS (upper portion of diagram) and SS (lower portion of diagram) boundaries of near CSL type according to their proximity to exact CSL matching and "specialness" (see text).

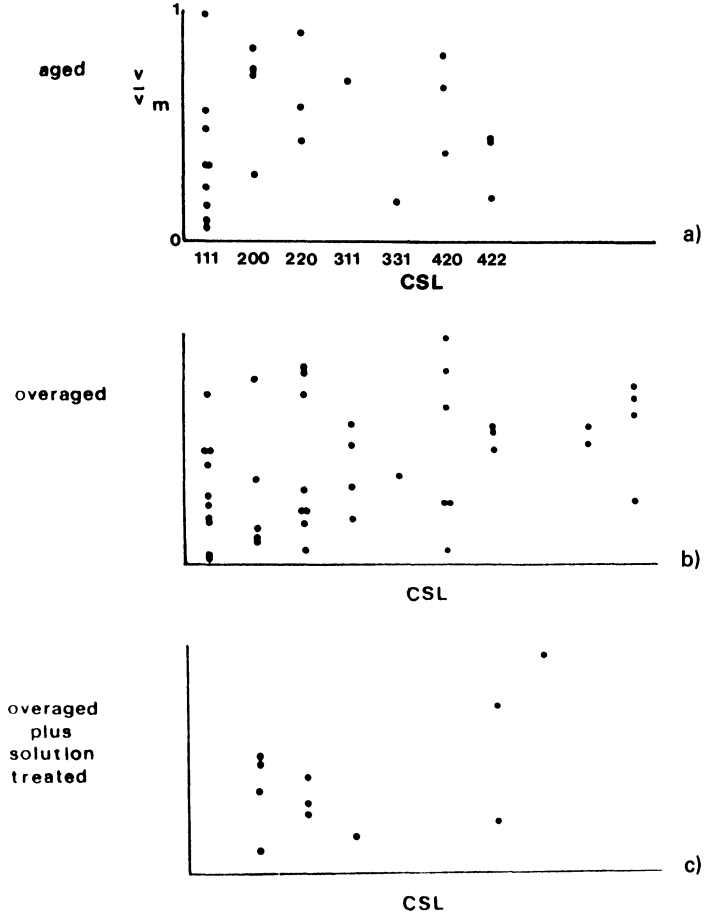

Figure 8 Diagram showing the distributions of CSLs according to their proximity to exact CSL matching (v/v_m) and the axis of rotation for a) aged, b) overaged and c) overaged plus solution-treated PE 16.

Furthermore, Figure 8 indicates that the CSLs from the overaged, strongly pinned specimens were nearer to exact coincidence (i.e. v/v_m approaches 0) than those from sets (1) and (3). The interpretation of this data is that the pinned boundaries, under the influence of thermal activation during the overaging treatment are able to rotate towards lower energy, i.e. geometrically special configurations (Randle and Ralph 1986b; Randle and Ralph 1987c).

Table 3 Proportions of CSL boundaries ($\Sigma \leqslant 49$) in sample populations from aged, overaged and overaged plus solution-treated PE16.

Specimen	% CSL boundaries
aged ($\gamma' \simeq 10$ nm)	27
overaged ($\gamma' \simeq 150$ nm)	47
overaged plus solution-treated (γ' absent)	17

GRAIN MISORIENTATION TEXTURE SIMULATIONS

Much insight into the macrotexture of materials has arisen from computer simulation (e.g. Abbruzzese and Lücke, 1986) This process permits a deeper level of interpretation to be offered as to the origins of experimentally derived textures. In the present section a first stage in the simulation of microtextural (GMT) data is described.

From the foregoing section, it is apparent that the relationship between the microtexture and the GMT distribution of special boundaries is a complex function of both geometrical constraints and other factors such as the preferential selection of certain boundaries on the grounds of low energy, high mobility, segregation and boundary interactions during migration. The selection of boundaries purely on the basis of probability can be simulated quite simply by picking orientations of grain pairs at random and computing the resultant axis/angle pair. For each grain three orthogonal unit vectors [*hkl*], [*uvw*], and [*abc*] are required to specify the orientation, *h*, *k*, *l* and *u* are chosen at random and multiplied by ± 1 at random. *v* and *w* are found by solving the following simultaneous equations:

$$hu + kv + lw = 0$$
$$u^2 + v^2 + w^2 = 1$$

and [*abc*] is obtained from the cross-product of [*hkl*] and [*uvw*].

The first row of Table 4 shows the result of the simulation of axis/angle pairs for random grain pairs. The proportion of $\Sigma \leqslant 19$

Table 4 Proportions of special boundaries (%) arising from over 2000 computer generated grain pairs of random orientation (first row) and four different microtextures. The CSL ($\Sigma \leqslant 37$) categorisation is further subdivided to show distributions of 100, 110 and 111 misorientation axes. Low angle (L) and medium angle (M) types are also recorded.

Texture	L 0–15°	M 15–20°	CSL $\Sigma \leqslant 37$	100	110	111	CSL $\Sigma \leqslant 19$
random	2.8	4.2	12.5	(6.9	36.2	44.8)	9.7
111	17.1	12.5	10.7	(6.7	20.0	56.7)	7.5
100	13.5	10.6	18.8	(100	0	0)	16.3
111/100 "*a*-type"	13.4	8.1	10.7	(53.7	14.7	18.9)	8.4
124 "*b*-type"	3.5	9.8	14.1	(8.4	28.6	31.4)	7.0

CSLs and the proportion of low angle boundaries agrees with the calculated figure and also with the figure obtained by random generation of axis/angle pairs (9%) (Warrington and Boon, 1975). [The present authors use a method to calculate the deviation of a boundary from the nearest CSL which measures the angles between the ⟨100⟩, ⟨010⟩ and ⟨001⟩ direction pairs in the experimental and reference boundary and records an average value, rather than accepting the deviation as the largest of these three angles (Randle and Ralph, 1986). Hence a slightly smaller value for the angular deviation from exact an CSL is obtained here, which may account for the slightly higher proportion of $\Sigma \leqslant 19$ CSLs compared to Warrington's value (9.7% c.f. 9.0%)].

Also included in Table 4 are the effects of imposing a texture on the choice of grain pair orientations. The limitations imposed are that only poles which are 10° from 111, 100, either 111 or 100, and 124 respectively are selected. The texture is restricted to one direction in each grain only, so as to simulate a fibre texture. For the first two texture cases, 100 and 111, the differences are very striking the ⟨100⟩ grain texture results in a sharp texture in the GMT (Figure 9) with an increase in both low and medium angle boundaries, and CSLs, all of which are misoriented around ⟨100⟩. The ⟨111⟩ texture does not produce such clear cut effects; although there is a greater increase in low and medium angle boundaries, the proportion of CSLs falls below that expected for a random

Figure 9 Simulated GMT plot from grain pairs whose grain normals are $\leq 10°$ from $\langle 100 \rangle$.

distribution (Table 4, row 1). Furthermore, only half the CSLs are misoriented about $\langle 111 \rangle$.

The purpose of the final two texture groups in Table 4—the 111/100 dual texture and the 124 texture, is to simulate respectively the *a* and *b* textures recorded from PE16. It is clear from comparisons of both Table 2 with Table 4, and Figure 6 with Figure 10, that the real GMT from PE16 is not governed by random geometric selection, since the distribution of boundary types is very different. The proportions of CSLs in the experiment are almost double the theoretical values, and furthermore, the CSLs in the experimental case are almost exclusively those CSLs which are associated with special properties and misoriented around 111 or 110 rather than predominantly around 100 as predicted. Clear evidence is thus provided that special grain boundaries are a preferred configuration, and polycrystalline aggregates with the microtextures described here will exhibit GMTs which are influenced by the high proportion of special boundaries.

There is an obvious reservation that must be placed upon the simulation/experimental GMT comparisons described above, namely that the simulations include only isolated grain pairs, whereas the experimental work relates to an assembly of connected grains. This connectivity will necessarily restrict the choice of available misorientations. Where boundary migration is occurring, if a high proportion of twin boundaries ($\Sigma = 3$) are already established, it is likely that these boundaries will interact to increase the proportions of $\Sigma 3$, $\Sigma 9$ and $\Sigma 27$ types if the reaction is

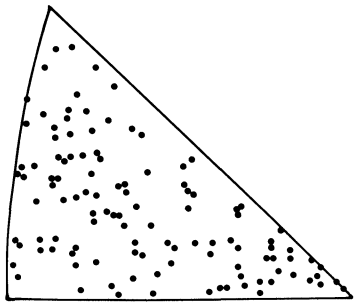

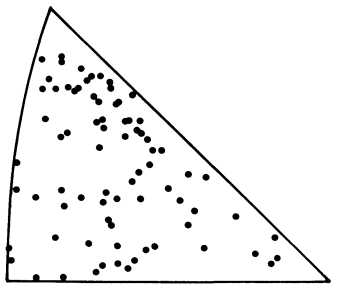

Figure 10 Simulated GMT plots from a) mixed 111/100 texture (i.e. grain orientations could be 10° from either ⟨111⟩ or ⟨100⟩) and b) 124 texture (grain orientations 10° from 124). Thus the GMTs from *a*-type and *b*-type textures are simulated.

energetically favourable (Goodhew, 1979)

$$\Sigma 3 + \Sigma 3 \rightarrow \Sigma 9$$

$$\Sigma 3 + \Sigma 9 \rightarrow \Sigma 27.$$

The other commonly observed CSLs, e.g. Σ11 and Σ19a may be perpetuated by a similar mechanism.

CONCLUDING REMARKS AND SUMMARY

1. Microtextural measurements refer to grain specific orientational data. This type of approach to preferred orientation highlights subtle aspects of a material's texture.

2. Microtextural data from contiguous grains also makes available the grain misorientation texture, GMT.

3. Two techniques are described for the acquisition of microtextures/GMTs, namely electron backscattering and convergent beam electron diffraction. The former technique is the quicker and more versatile for most applications.

4. Some examples of the collection and analysis of GMT data are overviewed. Since there is a growing awareness of the potential for designing materials with improved properties by control of grain boundary parameters, the analysis of GMTs, particularly in relation to proportions of special boundaries is a very important area of research.

5. Computer simulations of GMTs for non-textured and textured cases are presented. The proportions of special boundaries measured experimentally are both greater and varying in distribution of misorientation axis compared to the simulation.

Acknowledgements

One of us (VR) wishes to acknowledge the award of a research fellowship from the S.E.R.C., during the tenure of which this study was performed. The authors are grateful to Mr. R. D. Stacey of the Springfield Laboratories of the UKAEA for the supply of material, and to Dr. D. Dingley of the Physics Department of Bristol University for allowing access to his EBS equipment.

References

Abbruzzese, G. and Lücke, K. (1986) Proc. Int. Risø Symp. *Annealing* (eds. N. Hansen *et al.*) (Risø, Press, Denmark) 1–14.

Bunge, H. J. (1986) *Texture Analysis in Materials Science*: *Mathematical Methods* (Butterworths, London). (1982)

Bunge, H. J. and Dahlem, E. (1986) Proc. Int. Risø Symp. Annealing (eds. N. Hansen *et al.*) (Risø Press, Denmark) 255–260.

Bouchet, D. and Priester, L. (1987) *Scripta Met* **21**, 475–478.

Dechamps, M., Marrouch, A. Barbier, F. and Revcolevschi A. (1985) *J. de Phys.*, **46**, C4–435–440.

Dingley, D. J. (1984) *Scanning electron microscopy,* **2**, 569–575.

Goodhew, P. J. (1979) *Met. Sci.*, **13**, 108–112.

Grant, E., Juul Jensen, D. and Ralph, B. (1986) *J. Mat. Sci.*, **21**, 1688–1692.

Hartherley, M. and Hutchinson, W. B. (1979) *An Introduction to Textures in Metals*, (Institution of Metallurgists, London).
Honeycombe, R. W. K. (1979) *The Plastic Deformation of Metals,* (Edward Arnold (Publishers) Ltd.)
Howell, P. R., Fleet, D. E., Welch, P. I. and Ralph, B. (1978) *Acta Met.*, **26,** 1499–1503.
Inoko, F. (1986) Proc. Inst. Risø Symp. *Annealing* (eds. N. Hansen *et al.*) (Risø Press, Denmark) 373–378.
Mackenzie, J. K. (1964) *Acta Met.* **12**, 223–225.
Pumphrey, P. H. (1976) In: *Grain Boundary Structure and Properties*, (ed. G. A. Smith) p. 139.
Ractliffe, J.F. (1967) *Elements of Mathematical Statistics*, Oxford University Press.
Randle, V. and Ralph, B. (1985) Int. Phys. Conf. Ser. No. 78, EMAG '85, Adam Hilger, Bristol, p. 59.
Randle, V. and Ralph, B. (1986a) *J. Math. Sci.*, **21,** 3823–3828.
Randle, V. and Ralph, B. (1986b) In: Proc. 7th Risø Int. Symp. Denmark, 507–514.
Randle, V. and Ralph, B. (1987a) In: Mechanics and Mechanisms of Plasticity, *J. de Phys.*, in press.
Randle, V. and Ralph, B. (1987b) Proc. Roy. Soc., in press.
Randle, V. and Ralph, B. (1987c) *J. Mat. Sci.*, in press.
Randle, V. and Ralph, B. and Dingley, D. J. (1987) *Acta Met.*, in press.
Sickafus, K. E. and Sass, S. L. (1987) *Acta Met.*, **35,** 69–79.
Warrington, D. H. and Boon, M. (1975) *Acta Met.*, **23,** 599–607.
Watanabe,T., (1984) *Res. Mech.*, **11,** 47–84.